AIP | Journal of Applied Physics

Narrow-bandwidth solar upconversion: Case studies of existing systems and generalized fundamental limits

Justin A. Briggs, Ashwin C. Atre, and Jennifer A. Dionne

Citation: Journal of Applied Physics **113**, 124509 (2013); doi: 10.1063/1.4796092
View online: http://dx.doi.org/10.1063/1.4796092
View Table of Contents: http://scitation.aip.org/content/aip/journal/jap/113/12?ver=pdfcov
Published by the AIP Publishing

Narrow-bandwidth solar upconversion: Case studies of existing systems and generalized fundamental limits

Justin A. Briggs,[1,2,a)] Ashwin C. Atre,[2] and Jennifer A. Dionne[2]
[1]*Department of Applied Physics, Stanford University, 348 Via Pueblo Mall, Stanford, California 94305-4090, USA*
[2]*Department of Materials Science and Engineering, Stanford University, 496 Lomita Mall, Stanford, California 94305-4034, USA*

(Received 29 January 2013; accepted 6 March 2013; published online 29 March 2013)

Upconversion of sub-bandgap photons is a promising approach to exceed the Shockley-Queisser limit in solar technologies. Calculations have indicated that ideal, upconverter-enhanced cell efficiencies can exceed 44% for non-concentrated sunlight, but such improvements have yet to be observed experimentally. To explain this discrepancy, we develop a thermodynamic model of an upconverter-cell considering a highly realistic narrow-band, non-unity-quantum-yield upconverter. As expected, solar cell efficiencies increase with increasing upconverter bandwidth and quantum yield, with maximum efficiency enhancements found for near-infrared upconverter absorption bands. Our model indicates that existing bimolecular and lanthanide-based upconverters will not improve cell efficiencies more than 1%, consistent with recent experiments. However, our calculations show that these upconverters can significantly increase cell efficiencies from 28% to over 34% with improved quantum yield, despite their narrow bandwidths. Our results highlight the interplay of absorption and quantum yield in upconversion, and provide a platform for optimizing future solar upconverter designs. © *2013 American Institute of Physics*.
[http://dx.doi.org/10.1063/1.4796092]

In one hour, the sun delivers enough energy to the earth to meet global needs for an entire year.[1] However, semiconductor-based solar technologies are generally unable to utilize photons below the device bandgap and can thus harvest only a small portion of this energy. Spectral upconverters (UCs) provide a possible solution. Placed behind a cell, they capture transmitted sub-bandgap photons and convert them to a frequency range that can be utilized by the cell. Because they are electrically decoupled from the cell, they neither introduce recombination pathways for electron-hole pairs (as intermediate level systems do[2–4]), nor require current matching (as multi-junction systems do[5–7]). Upconversion has been observed in many systems, including rare earth and transition metal ions,[8–11] various semiconductor quantum dots,[12–14] and metallated macrocycles.[15–19] Further, upconversion quantum efficiencies greater than 20% have been reported for solid state systems under low-power, non-coherent illumination.[20] To date, upconverters have been successfully incorporated into many photovoltaic systems, including crystalline silicon,[21] amorphous silicon,[22] dye-sensitized,[23,24] and organic[25] solar cells, but efficiency enhancements have been small.

Trupke *et al*. considered the theoretical solar cell efficiency improvements possible with the addition of an ideal upconverter,[26,27] demonstrating efficiencies beyond the Shockley-Queisser limit. A further analysis accounted for cell non-idealities and a non-radiative relaxation pathway in the upconverter, indicating that solar concentration is not necessary to achieve substantial improvements in efficiency.[28] A recent study examined the impact of an idealized upconverter on a highly realistic crystalline silicon solar cell.[29] While these works assumed that the upconverter was able to absorb over the entire sub-bandgap spectrum, all known upconverters are found to absorb and emit radiation in relatively narrow bands, typically between 0.1 and 0.2 eV.[18,20,34] It is necessary to consider this practical limitation in order to accurately predict the efficiency enhancements afforded by upconversion.

Here, we theoretically study a solar cell with an upconverter characterized by narrow-band absorption and emission. We investigate the expected efficiency limits of a highly realistic solar cell-upconverter system, both optimizing upconverter design for a given cell bandgap and exploring the efficiencies possible with existing and next-generation upconversion systems. Current state-of-the-art upconverting materials are predicted to increase solar cell efficiency by almost one absolute percent, while emerging technologies are expected to boost efficiencies by several absolute percent.

We consider an ideal single-junction solar cell with an electrically isolated upconverter behind it, as depicted in Fig. 1(a). The upconverter is modeled as two low bandgap solar cells (C_3 and C_4) in series with a high bandgap photodiode (C_2).[26] As seen in Fig. 1(b), electrons excited by low energy photons in the low bandgap cells drive the photodiode into forward bias, allowing it to radiate above-bandgap photons. A generalized Planck radiation law[31] is used to describe the photon flux density emanating from the solar cell, the upconverter, the sun, and the ambient environment

$$j(T,\mu,\varepsilon,\hbar\omega) = \frac{\varepsilon}{4\pi^3\hbar^3c^2}\frac{(\hbar\omega)^2}{\exp\left(\frac{\hbar\omega-\mu}{kT}\right)-1}. \quad (1)$$

a)Author to whom correspondence should be addressed. Electronic mail: jabriggs@stanford.edu

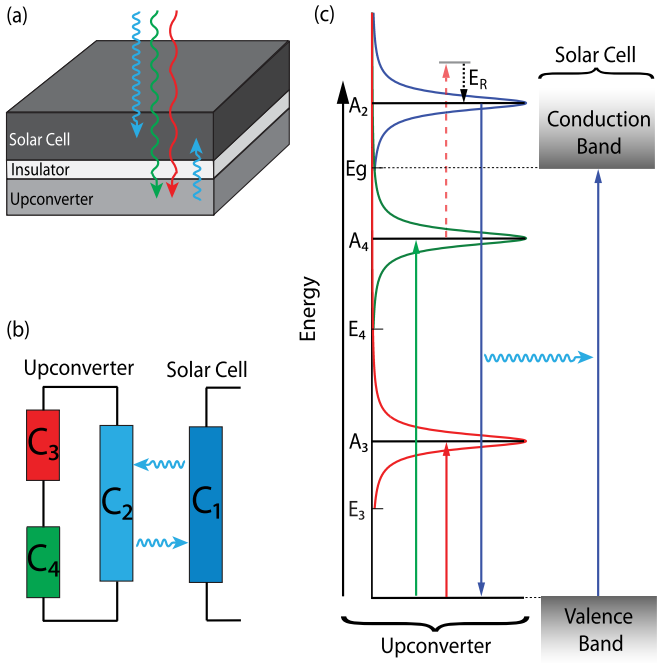

FIG. 1. Schematics outlining the solar cell/upconverter system under consideration. (a) Above-bandgap light is absorbed by the solar cell, which is electrically isolated from the upconverter. Sub-bandgap light is transmitted by the solar cell, absorbed by the upconverter, and re-radiated back into the cell as above-bandgap light. (b) The upconverter is equivalent to a circuit containing two low bandgap solar cells (C_3 and C_4) in series with a high bandgap photodiode (C_2). (c) Energy level diagram indicating the relevant transitions. E_g, E_3, and E_4 represent the effective band edges for cells C_2, C_3, and C_4, respectively (E_g is also the solar cell bandgap). A_2, A_3, and A_4 are the centroids of the upconverter emission and absorption lorentzians; the absorption and emission peaks for each cell comprising the upconverter (C_2, C_3, and C_4) are coincident, thus allowing the non-radiative relaxation energy E_R to account for all non-radiative loss in the upconverter. The solar cell conduction and valence bands extend to positive and negative infinity, respectively.

Here, $\hbar$ is the reduced Planck's constant, c is the speed of light in vacuum, T is the temperature of the radiating body, μ is the operating voltage of the body times the elementary charge, and ϵ is the étendue factor accounting for geometrical concentration of light and reflection from interfaces with mismatched refractive indices.[30]

To enforce the narrow-band absorption and emission characterizing known upconverters, we impose a spectral weighting lorentzian function $f(A, W; \hbar\omega)$, parameterized by a centroid A and a full width at half max W. The photon fluxes, $\dot{N}_i$, from each cell comprising the upconverter are computed as the convolution of the Planck distribution with this weighting function

$$\dot{N}_i(E_l, E_u, T_i, \mu_i, A_i, W_i, \epsilon) = \int_{E_l}^{E_u} j(T_i, \mu_i, \epsilon, \hbar\omega) f(A_i, W_i; \hbar\omega) d(\hbar\omega). \quad (2)$$

Here, the subscript i refers to the ith cell and E_l and E_u are the lower and upper bounds of the appropriate energy band of the ith cell. Photon fluxes from the sun, the environment, and the solar cell are given directly by the integral of the spectral density

$$\dot{N}_i(E_l, E_u, T_i, \mu_i, \epsilon) = \int_{E_l}^{E_u} j(T_i, \mu_i, \epsilon, \hbar\omega) d(\hbar\omega). \quad (3)$$

An energy level diagram representing the resulting three-level, narrow-band system is shown in Fig. 1(c). We assume that all non-radiative losses in the system are accounted for by a single relaxation energy parameter, E_R. As such, A_2, A_3, and A_4 represent the centroids of the emission and absorption lorentzians associated with cells C_2, C_3, and C_4. The parameters E_g, E_3, and E_4 represent the effective band edges associated with the upconverter transitions, and thus define the lower bounds of integration when Eq. (2) is applied to the cells comprising the upconverter, C_2, C_3, and C_4 (E_g is also the solar cell bandgap). Conservation of energy dictates that $A_3 + A_4 - E_R = A_2$, where E_R is the non-radiative relaxation energy. We assume that the bandwidths of all absorption and emission processes in the upconverter are equal, and refer to this value as the upconverter bandwidth. To ensure good optical coupling between the upconverter and the solar cell, we select an upconverter emission energy A_2 that is sufficiently above (>0.1 eV) the cell bandgap (see supplementary material for a detailed description[43]).

This model captures the essential optical behavior exhibited by known upconverters. While the generalized Planck distribution gives the nominal photon flux density resulting from Fermionic transitions in any material at a given temperature and potential, it does not account for the density of Fermionic states in that material. In order to account, for example, for the sharp density of electronic states in an ensemble of atomic or molecular emitters, one must impose a further modulation of the optical output. The convolution of the lorentzian weighting function with the generalized Planck distribution achieves this modulation, thus effectively modeling the narrow-band optical response of existing upconverting materials.

We employ a generalization of the detailed balance approach used by Shockley and Queisser.[26,32,33] In this model, the current density in the ith cell is equal to the elementary charge times the difference between the photon fluxes absorbed and emitted by that cell

$$I_i = q(f_{abs,i}\dot{N}_{inc,i} - f_{rec,i}\dot{N}_{em,i}), \quad (4)$$

where $f_{abs,i}$ and $f_{rec,i}$ are the absorption efficiency and the inverse of the radiative recombination efficiency of the ith cell[28] (see supplementary material[43] for detailed equations). The absorption efficiency gives the fraction of incident photons that are absorbed. The radiative recombination efficiency gives the fraction of recombination events in a cell that are radiative, so, for example, $f_{rec,i} = 10\%$ implies that for every electron-hole pair that radiatively recombines in the ith cell, ten pairs will non-radiatively recombine.

These efficiency parameters are closely related to the quantum efficiency of the solar cell and the upconverter. The quantum efficiency, or quantum yield, of the solar cell is defined as the ratio of extracted electrons to incident photons. Analogously, the upconverter quantum efficiency is defined as the number of high energy photons emitted for every pair of incident low energy photons. Even when the

solar cell has $f_{abs,1} = f_{rec,1} = 1$, it does not technically have unity quantum yield because electron-hole pairs can still radiatively recombine, thus diminishing the number of extracted electrons. Similarly, radiative recombination in cells C_3 and C_4 will result in non-unity unconverter quantum efficiency even when $f_{abs,i} = f_{rec,i} = 1$ for $i = 2$, 3, and 4. However, the photon fluxes resulting from this radiative recombination are many orders of magnitude smaller than other relevant fluxes (e.g., flux from the sun or cell C_2 when it is driven into forward bias). As such, a solar cell with $f_{abs,1} = f_{rec,1} = 1$ effectively has unity quantum efficiency, and we consider this cell to be ideal. Similarly, an ideal upconverter is considered to be one with $f_{abs,i} = f_{rec,i} = 1$ for $i = 2$, 3, and 4 because it effectively has unity upconverter quantum efficiency.

Using the above thermodynamic model and detailed balance equations, we optimize the solar cell efficiency as a function of the upconverter absorption peak positions and the operating potentials of the solar cell and upconverter cells. This optimization is subject to the series circuit constraints placed on the currents and operating potentials of the cells comprising the upconverter: $I_2 = -I_3 = -I_4$ and $\mu_2 = \mu_3 + \mu_4$.

We begin by assuming both the solar cell and the upconverter have unity absorption and radiative recombination efficiencies, and that the sun and the ambient environment are ideal blackbody emitters at 6000 K and 300 K, respectively. We calculate the maximum power conversion efficiency of this idealized system as a function of cell bandgap and upconverter bandwidth (Fig. 2(a)). In the limit of zero bandwidth, i.e. no upconversion, the Shockley-Queisser limit is recovered, giving 30.6% cell efficiency at a bandgap of 1.3 eV. As the bandwidth increases, the peak efficiency increases and the cell bandgap at which this maximum is achieved blueshifts. The addition of ideal 0.1 eV, 0.3 eV, and 0.5 eV bandwidth upconverters to an ideal 1.7 eV bandgap solar cell (characteristic of amorphous silicon and some organic photovoltaics) results in an efficiency increase from 28.2% to 33.5%, 39.9%, and 43.6%, respectively. As 0.5 eV is approximately an upper limit for the bandwidth of known upconverters, this latter value represents the maximum expected efficiency enhancement possible with a lorentzian-band upconverter.

This analysis employs an optimized relaxation energy, which we compute to be 0.48 eV. Fig. 2(b) depicts the absolute increase in cell efficiency over the Shockley-Queisser curve as a function of upconverter relaxation energy for a 0.1 eV bandwidth upconverter. As seen, the optimal relaxation energy is largely independent of cell bandgap. As the upconverter bandwidth is increased, the optimal relaxation energy becomes smaller, but always lies between 0.35 and 0.5 eV for bandwidths between 0.1 and 0.5 eV (see supplementary material[43] for plot of absolute efficiency increase versus bandwidth for a range of bandgaps and bandwidths). These optimized values are within the relaxation energy range of typical upconverters which lose between 0.3 eV and 2.6 eV during upconversion.

Our narrow-bandwidth model allows us to optimize the spectral characteristics of an upconverter. To determine the ideal upconverter energy levels, we use the optimal relaxation energy of 0.48 eV and fix the upconverter bandwidth at 0.1 eV—a value meant to reflect the narrow absorption observed in existing upconverters. The solar cell efficiency is then optimized as a function of the spectral locations of the upconverter absorption peaks.

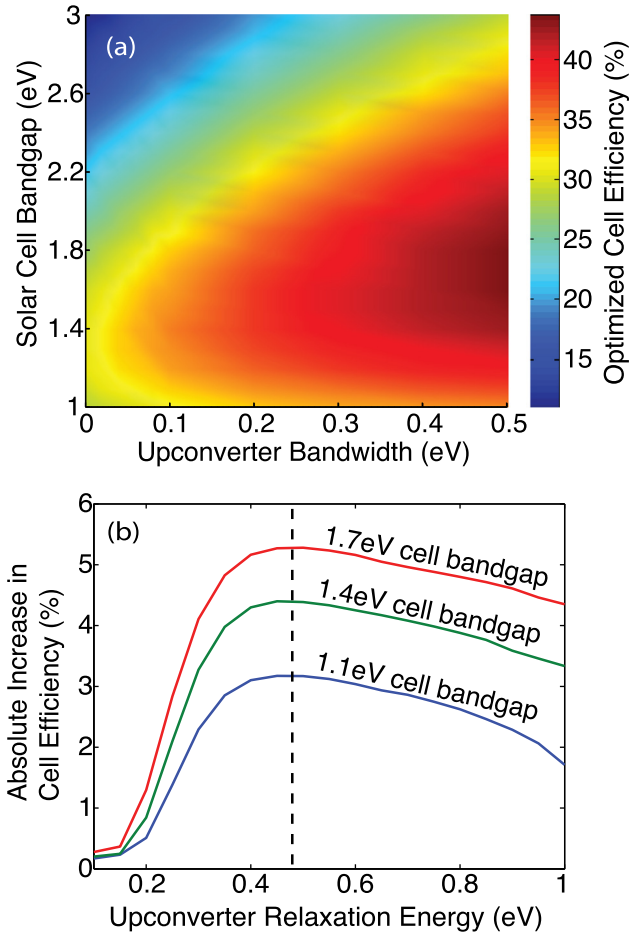

FIG. 2. Ideal solar cell with an ideal upconverter. (a) The maximum power conversion efficiency is calculated as a function of cell bandgap and upconverter bandwidth for the optimal relaxation energy of 0.48 eV. The Shockley-Queisser limit is thus generalized to include a narrow-band upconverter. (b) The absolute increase in cell efficiency is computed as a function of upconverter relaxation energy for a 0.1 eV bandwidth upconverter; the dotted line indicates the relaxation energy at which the maximum increase is achieved.

Figure 3 plots these ideal absorption energies using both the solar Planck distribution (fine lines) and the AM1.5 G solar irradiance spectrum[35] (thicker lines). As can be seen, the optimal upconverter absorption peaks in a general dual-absorber system tend to increase in energy with cell bandgap and are generally in the near-infrared. For example, for a 1.7 eV bandgap, the optimal absorption peaks lie at 1.0 eV and 1.5 eV. It is encouraging that these values are readily accessible with existing upconverters.[34,39] Note, however, that the ideal absorption positions depend on the absorption lines in the AM1.5G spectrum, as evidenced by the discrete energy jumps across solar absorption lines. This analysis serves as a design guide for future exploration of new upconverting systems.

As an application of our model, we explore the efficiency gains possible with the addition of two existing upconverters.

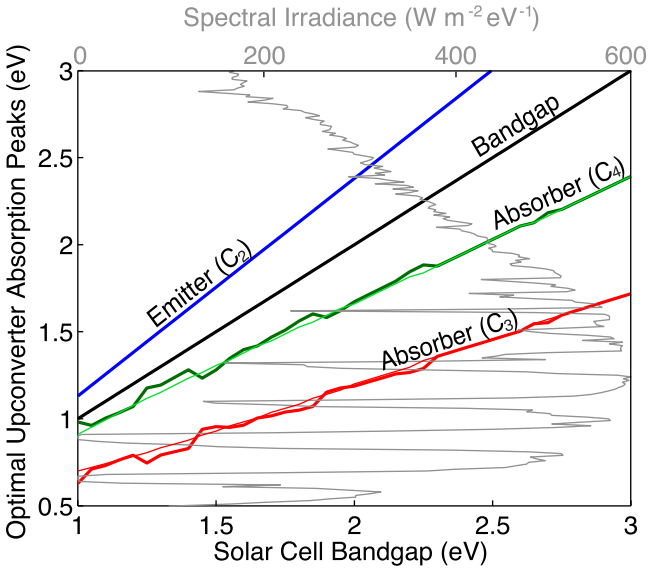

FIG. 3. Calculated optimal spectral locations for the low energy absorption peaks in the upconverter, determined using both the solar Planck spectrum (fine lines) and the AM1.5G solar irradiance spectrum (thicker lines). The emitter position is fixed relative to each bandgap. The AM1.5G spectrum is plotted (relative to the upper horizontal axis) for reference.

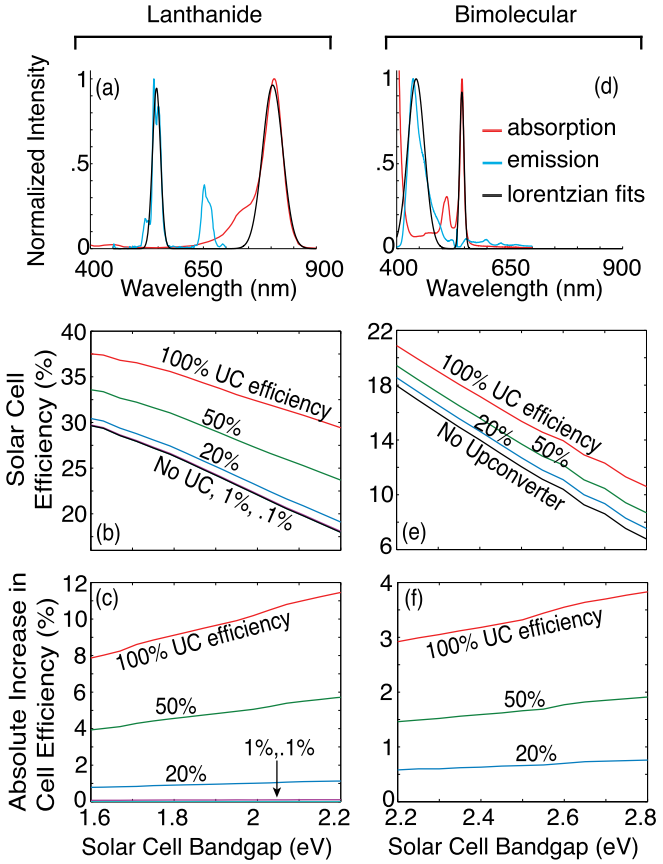

FIG. 4. Case studies of existing upconverting systems with different UC efficiencies are shown. The absorption and emission spectra and associated lorentzian fits (a), the raw efficiency (b), and the absolute increase in efficiency (c) for the bimolecular system (PdOEP + DPA). Analogous plots (d)–(f) for the lanthanide-based system (IR806-sensitized oleylamine-coated β-$NaYF_4$:Yb,Er nanoparticles). The axes in the bimolecular spectra plot extend to 900 nm for better spectral comparison.

We consider both a bimolecular system (the absorber Pd(II) octaethylporphyrin (PdOEP) paired with the emitter diphenylanthracene (DPA)),[20] and a lanthanide-based system (oleylamine-coated β-$NaYF_4$:Yb,Er nanoparticles sensitized with the carboxylated cyanine dye IR806).[34] We choose these upconverting materials because they show particular promise. The bimolecular system has achieved upconversion efficiencies over 20% in a solid polymer matrix and exhibits notable durability and longevity.[20] Lanthanide-based systems typically suffer from two major drawbacks: low quantum efficiency and spectrally narrow absorption. However, sensitization with the cyanine dye IR806 dramatically increases the absorption bandwidth of the lanthanide system,[34] significantly mitigating the latter disadvantage. Further, because these sensitized lanthanide-doped nanoparticles upconvert light from ~1.5 eV to ~2.3 eV, they are well suited for existing solar technologies with bandgaps lying between these values.

In our prior analyses, the solar cell efficiency was optimized as a function of the spectral positions of the upconverter absorption peaks; the maximum efficiencies reported are thus associated with optimal upconverter absorption peaks. In contrast, in these studies of specific upconverting systems, we employ lorentzian fits of empirical absorption and emission spectra to fix the absorption and emission lorentzians. The absorption and emission spectra of these two example systems, and the associated lorentzian fits used in the model, are illustrated in Figs. 4(a) and 4(d). While single lorentzian fits are not completely sufficient to capture all the complexity of the upconversion spectra, they are a good first approximation and provide a lower bound for upconverter absorption bandwidth due to the neglect of absorption peak shoulders and sidebands.

Figures 4(b), 4(c), 4(e), and 4(f) show efficiency enhancements as a function of bandgap for different upconverter efficiencies. The lowest upconverter efficiencies used in each plot represent recently measured values (20% for PdOEP/DPA[20] and 0.1% for the nanoparticle lanthanide-based system[34]); the curves labeled with higher upconverter efficiencies are meant to reflect the expected solar cell efficiency enhancements should ongoing work lead to more efficient upconversion.[36–39] Though non-ideal spectral positioning and low efficiencies limit current upconverters, these calculations highlight the promise of this technology. For example, application of the extant 20% efficient bimolecular upconverter to a 2.6 eV bandgap cell (useful, for example, for some photoelectrochemical devices[40]) would result in an increase in cell efficiency from 10.4% to 11.1%. If bimolecular upconversion efficiency could be increased to between 50% and 100%, the efficiency of the same cell would be boosted to between 12.1% and 14.0%. In contrast, application of the existing lanthanide-based nanoparticle system is not expected to enhance solar cell efficiency due to low upconverter quantum efficiencies. However, if lanthanide upconversion reaches quantum yields of 20%, 50%, or 100%, it is expected that the efficiency of a 1.7 eV bandgap solar cell would be boosted from 28.2% to 28.8%, 31.3%, or 34.4%, respectively. Several recently developed lanthanide systems show promise for achieving such quantum yields.[41,42]

We have investigated the effects of narrow-band upconversion on the efficiency of a solar cell. Generalizing the Shockley-Queisser limit, we determined that the addition of an ideal upconverter with absorption bandwidth between 0.1 eV and 0.5 eV should boost the efficiency of a 1.7 eV bandgap cell from 28.2% to between 33.5% and 43.6%. Further, we found that the optimal absorption peaks for such an upconverter lie at 1.0 eV and 1.5 eV, and similarly mapped out the optimal upconverter parameters for any given cell bandgap. Our case studies indicate that bimolecular upconverting materials are already well-suited to enhance the efficiency of high-bandgap devices by almost one absolute percent, but that dye-sensitized lanthanide-based systems are not yet viable due to their low quantum efficiencies. However, should upconverter quantum yields be boosted beyond their current values, cell efficiency enhancements of several absolute percent are predicted for both systems. These calculations highlight the promise of upconversion for photovoltaics and stress the critical roles of upconverter absorption bandwidth and quantum yield in the push towards technological viability.

We thank Michael McGehee, Alberto Salleo, Tim Burke, Diane Wu, and Sacha Verweij for insightful discussions. Funding for this research was provided by the Department of Energy under Grant No. DE-EE0005331, Stanford's TomKat Center for Sustainable Energy, Stanford Global Climate and Energy Project (GCEP), the Robert L. and Audrey S. Hancock Stanford Graduate Fellowship, and the National Science Foundation Graduate Research Fellowship under Grant No. 2012122469. Any opinion, findings, and conclusions or recommendations expressed in this material are those of the authors and do not necessarily reflect the views of the National Science Foundation.

[1]N. Lewis and D. Nocera, Proc. Natl. Acad. Sci. U.S.A. **103**, 15729 (2006).
[2]M. Keevers and M. Green, J. Appl. Phys. **75**, 4022 (1994).
[3]A. Luque and A. Martí, Phys. Rev. Lett. **78**, 5014 (1997).
[4]G. Güttler and H. Queisser, Energy Convers. **10**, 51 (1970).
[5]R. King, D. Law, K. Edmondson, C. Fetzer, G. Kinsey, H. Yoon, R. Sherif, and N. Karam, Appl. Phys. Lett. **90**, 183516 (2007).
[6]J. Geisz, D. Friedman, J. Ward, A. Duda, W. Olavarria, T. Moriarty, J. Kiehl, M. Romero, A. Norman, and K. Jones, Appl. Phys. Lett. **93**, 123505 (2008).
[7]W. Guter, J. Schöne, S. Philipps, M. Steiner, G. Siefer, A. Wekkeli, E. Welser, E. Oliva, A. Bett, and F. Dimroth, Appl. Phys. Lett. **94**, 223504 (2009).
[8]M. Pollnau, D. Gamelin, S. Lüthi, H. Güdel, and M. Hehlen, Phys. Rev. B **61**, 3337 (2000).
[9]S. Heer, K. Kömpe, H. Güdel, and M. Haase, Adv. Mater. **16**, 2102 (2004).
[10]J. Boyer, L. Cuccia, and J. Capobianco, Nano Lett. **7**, 847 (2007).
[11]F. Auzel, Chem. Rev. **104**, 139 (2004).
[12]X. Wang, W. Yu, J. Zhang, J. Aldana, X. Peng, and M. Xiao, Phys. Rev. B **68**, 125318 (2003).
[13]E. Poles, D. Selmarten, O. Mićić, and A. Nozik, Appl. Phys. Lett. **75**, 971 (1999).
[14]C. Bonati, A. Cannizzo, D. Tonti, A. Tortschanoff, F. van Mourik, and M. Chergui, Phys. Rev. B **76**, 033304 (2007).
[15]S. Baluschev, T. Miteva, V. Yakutkin, G. Nelles, A. Yasuda, and G. Wegner, Phys. Rev. Lett. **97**, 143903 (2006).
[16]S. Baluschev, V. Yakutkin, G. Wegner, T. Miteva, G. Nelles, A. Yasuda, S. Chernov, S. Aleshchenkov, and A. Cheprakov, Appl. Phys. Lett. **90**, 181103 (2007).
[17]V. Yakutkin, S. Aleshchenkov, S. Chernov, T. Miteva, G. Nelles, A. Cheprakov, and S. Baluschev, Chem.-Eur. J. **14**, 9846 (2008).
[18]T. Singh-Rachford and F. Castellano, Coord. Chem. Rev. **254**, 2560 (2010).
[19]R. Islangulov, J. Lott, C. Weder, and F. Castellano, J. Am. Chem. Soc. **129**, 12652 (2007).
[20]J.-H. Kim, F. Deng, F. N. Castellano, and J.-H. Kim, Chem. Mater. **24**, 2250 (2012).
[21]A. Shalav, B. S. Richards, T. Trupke, K. W. Krämer, and H. U. Güdel, Appl. Phys. Lett. **86**, 013505 (2005).
[22]J. de Wild, J. K. Rath, A. Meijerink, W. G. J. H. M. van Sark, and R. E. I. Schropp, Sol. Energy Mater. Sol. Cells **94**, 2395 (2010).
[23]G.-B. Shan and G. P. Demopoulos, Adv. Mater. **22**, 4373 (2012).
[24]C. Yuan, G. Chen, P. N. Prasad, T. Y. Ohulchanskyy, Z. Ning, H. Tian, L. Sund, and H. Ågren, J. Mater. Chem. **22**, 16709 (2012).
[25]H.-Q. Wang, M. Batentschuk, A. Osvet, L. Pinna, and C. J. Brabec, Adv. Mater. **23**, 2675 (2011).
[26]T. Trupke, M. Green, and P. Würfel, J. Appl. Phys. **92**, 4117 (2002).
[27]T. Trupke, A. Shalav, B. S. Richards, P. Würfel, and M. A. Green, Sol. Energy Mater. Sol. Cells **90**, 3327 (2006).
[28]A. C. Atre and J. A. Dionne, J. Appl. Phys. **110**, 034505 (2011).
[29]C. M. Johnson and G. J. Conibeer, J. Appl. Phys. **112**, 103108 (2012).
[30]V. Badescu, A. Vos, A. Badescu, and A. Szymanska, J. Phys. D **40**, 341 (2007).
[31]P. Würfel, J. Phys. C **15**, 3967 (1982).
[32]W. Shockley and H. Queisser, J. Appl. Phys. **32**, 510 (1961).
[33]V. Badescu, J. Appl. Phys. **104**, 113120 (2008).
[34]W. Zou, C. Visser, J. A. Maduro, M. S. Pshenichnikov, and J. C. Hummelen, Nature Photon. **6**, 560 (2012).
[35]National Renewable Energy Laboratory, see http://rredc.nrel.gov/solar/spectra/am1.5/ for the spectral data used in this work.
[36]A. C. Atre, A. García-Etxarri, H. Alaeian, and J. A. Dionne, J. Opt. **14**, 024008 (2012).
[37]M. Saboktakin, X. Ye, S. J. Oh, S.-H. Hong, A. T. Fafarman, U. K. Chettiar, N. Engheta, C. B. Murray, and C. R. Kagan, ACS Nano **6**, 8758 (2012).
[38]S. Schietinger, T. Aichele, H.-Q. Wang, T. Nann, and O. Benson, Nano Lett. **10**, 134 (2010).
[39]E. Verhagen, L. Kuipers, and A. Polman, Opt. Express **17**, 14586 (2009).
[40]M. Grätzel, Nature **414**, 338 (2001).
[41]S. K. W. MacDougall, A. Ivaturi, J. Marques-Hueso, K. W. Krämer, and B. S. Richards, Opt. Exp. **20**, A879 (2012).
[42]S. Fischer, J. C. Goldschmidt, P. Löper, G. H. Bauer, R. Brüggemann, K. Krämer, D. Biner, M. Hermle, and S. W. Glunz, J. Appl. Phys. **108**, 044912 (2010).
[43]See supplementary material at http://dx.doi.org/10.1063/1.4796092 for (1) a discussion of the energy levels and optimization routine used to model the upconversion process, (2) calculation of currents in each cell, (3) a discussion of the relationship between upconverter relaxation energy and upconverter bandwidth, (4) a table of the spectral parameters used to model upconversion in the bimolecular and lanthanide nanoparticle case studies, and (5) a brief note on solar cell non-idealities.